AFRL-RX-TY-TP-2011-0108

ENCLOSURE FIRE TESTS FOR UNDERSTANDING AIRCRAFT COMPOSITE FIRE ENVIRONMENTS

Alexander L. Brown and Amanda B. Dodd
Sandia National Labs
P.O. Box 5800
Albuquerque, NM 87185-1135

Brent M. Pickett
Air Force Research Laboratory
Airbase Technologies Division
139 Barnes Drive, Suite 2
Tyndall Air Force Base, FL 32403-5323

Contract No. FA4819-09-C-0030

June 2011

AIR FORCE RESEARCH LABORATORY
MATERIALS AND MANUFACTURING DIRECTORATE

■ **Air Force Materiel Command** ■ **United States Air Force** ■ **Tyndall Air Force Base, FL 32403-5323**

REPORT DOCUMENTATION PAGE

Form Approved
OMB No. 0704-0188

PLEASE DO NOT RETURN YOUR FORM TO THE ABOVE ADDRESS.

1. REPORT DATE *(DD-MM-YYYY)*	2. REPORT TYPE	3. DATES COVERED *(From - To)*
30-JUN-2011	POSTPRINT Journal Article	01-DEC-2010 -- 01-APR-2011

4. TITLE AND SUBTITLE

Enclosure Fire Tests for Understanding Aircraft Composite Fire Environments (POSTPRINT)

5a. CONTRACT NUMBER

FA4819-09-C-0030

5b. GRANT NUMBER

5c. PROGRAM ELEMENT NUMBER

6. AUTHOR(S)

* Brown, Alexander L.; * Dodd, Amanda B.; ** Pickett, Brent M.

5d. PROJECT NUMBER

5e. TASK NUMBER

5f. WORK UNIT NUMBER

QD103005

7. PERFORMING ORGANIZATION NAME(S) AND ADDRESS(ES)

* Sandia National Labs
P.O. Box 5800
Albuquerque, NM 87185-1135

8. PERFORMING ORGANIZATION REPORT NUMBER

9. SPONSORING/MONITORING AGENCY NAME(S) AND ADDRESS(ES)

** Air Force Research Laboratory
Materials and Manufacturing Directorate
Airbase Technologies Division
139 Barnes Drive, Suite 2
Tyndall Air Force Base, FL 32403-5323

10. SPONSOR/MONITOR'S ACRONYM(S)

AFRL/RXQES

11. SPONSOR/MONITOR'S REPORT NUMBER(S)

AFRL-RX-TY-TP-2011-0108

12. DISTRIBUTION/AVAILABILITY STATEMENT

Distribution A: Approved for public release; distribution unlimited.

13. SUPPLEMENTARY NOTES

Ref Public Affairs Case # 88ABW-2011-2606, 4 May 2011. Document contains color images.

14. ABSTRACT

Composite materials are increasingly being used in aviation applications and as the amount of composite material increases, there is a greater need to develop a better understanding of composite material response in fire environments. We have recently developed an experimental and computational program to examine this problem, with a focus on understanding duration, intensity, and the underlying physics during composite fires as well as the technology and procedures to safely manage composite fire events. In the past year, we have performed both small and intermediate scale tests to understand the behavior of composite materials used in aviation applications. The current focus is on a set of intermediate-scale tests that generates data useful for understanding the behavior of carbon fiber epoxy composites in adverse thermal environments. Intermediate scale tests help bridge the gap of understanding between small-scale experimental efforts and practical scale problems.

Our intermediate-scale tests are expected to result in a thermally extreme environment that may be representative of an intense fire scenario. The test set-up involves a 91 cm cubic enclosure, instrumented to measure heat flux, gas species, velocity, and temperature. Features of the enclosure include controlled air aspiration, insulated walls, and gas burners to ignite the composite materials placed therein. The floor of the enclosure is loaded with 22.7 to 45.4 kg (50 to 100 lbs) of material. Propane burners are used to ignite the solid materials during the first few minutes of the test. The remainder of the test involves sustained combustion of the composite materials. Preliminary results provide information on the severity of the environment both in terms of thermal intensity and chemical products.

15. SUBJECT TERMS

enclosure, composite fire, heat flux, temperature

16. SECURITY CLASSIFICATION OF:			17. LIMITATION OF ABSTRACT	18. NUMBER OF PAGES	19a. NAME OF RESPONSIBLE PERSON
a. REPORT	b. ABSTRACT	c. THIS PAGE			Brent M. Pickett
U	U	U	UU	23	19b. TELEPHONE NUMBER *(Include area code)*

Reset

Standard Form 298 (Rev. 8/98)
Prescribed by ANSI Std. Z39.18

Enclosure Fire Tests for Understanding Aircraft Composite Fire Environments

Alexander L. Brown[1,3], Amanda B. Dodd[1], Brent M. Pickett[2]
[1]Sandia National Labs
[2]Air Force Research Laboratories
[3]Corresponding author addresses:
PO Box 5800
Albuquerque, NM 87185-1135 USA
albrown@sandia.gov

Prepared for:
CIF 6 Composites in Fire Conference
9-10 June 2011
University of Newcastle
Newcastle upon Tyne, UK
http://www.compositesinfire.com/

Abstract

Composite materials are increasingly being used in aviation applications and as the amount of composite material increases, there is a greater need to develop a better understanding of composite material response in fire environments. We have recently developed an experimental and computational program to examine this problem, with a focus on understanding duration, intensity, and the underlying physics during composite fires as well as the technology and procedures to safely manage composite fire events. In the past year, we have performed both small and intermediate scale tests to understand the behavior of composite materials used in aviation applications. The current focus is on a set of intermediate-scale tests that generates data useful for understanding the behavior of carbon fiber epoxy composites in adverse thermal environments. Intermediate scale tests help bridge the gap of understanding between small-scale experimental efforts and practical scale problems.

Our intermediate-scale tests are expected to result in a thermally extreme environment that may be representative of an intense fire scenario. The test set-up involves a 91 cm cubic enclosure, instrumented to measure heat flux, gas species, velocity, and temperature. Features of the enclosure include controlled air aspiration, insulated walls, and gas burners to ignite the composite materials placed therein. The floor of the enclosure is loaded with 22.7 to 45.4 kg (50 to 100 lbs) of material. Propane burners are used to ignite the solid materials during the first few minutes of the test. The remainder of the test involves sustained combustion of the composite materials. Preliminary results provide information on the severity of the environment both in terms of thermal intensity and chemical products.

Introduction

Composite materials are increasingly being used in the design of aircraft. They offer comparable structural strength to traditional metals such as aluminum and titanium for a fraction of the weight. These are positive consequences to this transition, as a weight savings can affect a fuel savings. Fuel savings reduce emissions, increase transportation efficiency, and reduce operating costs. There are negative

consequences as well. It is more costly to build aircraft with these materials. This cost is presumably offset by the fuel savings over the lifetime of the aircraft. Because composites are comparatively new, they have performance issues compared to metal structures. Lifetime strength, maintenance, and reliability issues are important performance consideration, and have been moderately well studied. There are other metrics of performance, such as the focus of this study, which is the concern of the environment resulting from an incident of a fire involving an aircraft with significant composite materials.

Aircraft fires are not an uncommon event. Airports have equipped and trained response personnel to help prevent loss of life and property. Response teams must be adequately trained and aware of safe and optimal methods to best perform their function, but not all fires occur in proximity to emergency fire fighters. There are remote events that may lead to aircraft fires that cannot be extinguished by a response team. Transportation safety can be improved when these environments are better understood.

Most aircraft composites consist of a binder and a fiber. These can vary widely in their characteristic behavior in a fire. Furthermore, lay-up of the materials is relevant, and there are numerous common configurations. Aircraft parts are typically made from layers of either unidirectional fibers oriented in varying relative rotational directionality or woven fabrics of similarly varying orientations. Pre-cure, the sheets are malleable, and can be formed into a variety of shapes. Lay-up patterns are customized according to engineering requirements, and typically vary throughout an aircraft. Various thicknesses are selected depending on design requirements. This results in a heterogeneous material that is often not easily characterized by traditional scalar properties applicable to homogeneous materials. The complexity of the part design methods challenges the ability to predict the outcome of a fire.

The behavior of composite materials in response to a fire has been studied previously by Tyson et al. [1986], Fanucci [1987], Brown et al. [1988], Levchik and Weil [2004], Mouritz [2006], Jiang et al. [2007], Quintiere et al. [2007], Delfa et al. [2009], Lopez de Santiago et al. [2010], and Hubbard et al. [2011]. This list does not include all of the research that has been done for composite materials, but highlights those authors who have studied carbon fiber epoxy composites, which are of interest in the current work. Jiang et al. [2007], Levchik and Weil [2004], and Fanucci, [1987] focused on thermal and/or decomposition behavior of the epoxy resins and carbon fiber epoxy composites. Brown et al. [1988] used the cone calorimeter to characterize ignitability and flammability of composite materials. Mouritz [2006] developed a database of fire properties of polymer composite materials for both aircraft cabin and aircraft structural materials. By gathering information from the literature, Mouritz [2006] reports the following fire properties as available: time-to–ignition, limiting oxygen index, peak heat release rate, average heat release rate, total heat release, flame spread rate, smoke, and combustion gases. Quintiere et al. [2007] studied the behavior of a carbon fiber epoxy composite through the use of cone calorimeter data, microscale combustion calorimeter data, thermogravimetric analysis, differential scanning calorimetry, Ohio State University (OSU) fire calorimeter tests, and a flame spread apparatus. Delfa et al. [2009] peformed small scale testing to evaluate the structural failure time of composite materials in a fire under a structural load. Tyson et al. [1986] performed an extensive study to examine

the response of two different graphite epoxy composite materials. Their studies on 1 foot square, 0.5 inch thick samples were designed to simulate the wing design of a modern fighter aircraft. They found that composites exhibited a greater burnthrough resistance than aluminum, but after the flames were extinguished, smoldering combustion was observed. Subsequent studies of the smoldering combustion processes revealed two types of smoldering: epoxy-smoldering (occurs in thick specimens around 400ºC and produces an exothermic reaction with its own supply of oxidizer) and carbon-fiber combustion (occurs after epoxy is consumed and after the temperature is "sufficiently high to sustain combustion of the individual fibers"). As a result, a subsequent study on fire-fighting techniques ensued. Four agents were examined: water, CO_2, potassium bicarbonate (purple k) and aqueous film-forming foam (AFFF) were tested. AFFF was the most effective.

In a previous test series where samples were exposed to 800ºC and 1000ºC radiative emitting panels, flaming combustion occurred for all the 1000ºC tests and for some of the 800ºC tests [Hubbard et al. 2011]. In these tests, there was no indication of fiber consumption. However, under conditions, it is expected that sustainable oxidation and combustion of the residual char and fibers will occur. Literature on the combustion of graphitic carbon suggests the need for fairly high temperatures to initiate the surface oxidation reactions (see for example Makino et al., [2003] and Babrauskas, [2003]).

In the current study, a test enclosure was designed and constructed to evaluate the severity of a fire environment involving composite materials. One objective is to achieve combustion of the fibers and to evaluate the burn duration. Another objective is to determine the magnitude of the thermal intensity that is created by the combustion of these materials. We are also concerned with the environmental hazards to personnel created by the burning of these materials, and hope to extract relevant data on the vapor and particulate products emitted from the fire. A final objective is to create and document the data in such a way that it may be useful for model comparison.

Methods

Because achieving a thermally extreme environment is one of the goals of this project, we have constructed a test enclosure that is expected to provide a unique set of data. We expect heat fluxes will be higher when compared to more common open burns, as we have designed the enclosure to provide insulation and isolation from the external environment in an effort to achieve peak sustained fluxes. The insulated walls are nearly adiabatic, and will augment the re-radiation compared to more conductive materials.

Materials

Because of the high cost of the composite material, performing large tests is difficult. For this test series, we have acquired an array of pieces from which we formulated a test matrix. Ideally, highly relevant material types and shapes would be used, but because the quantities of perfect material were not readily obtainable, a compromise was made by testing materials that were readily available, with binder and fiber relevancy, and with shapes that were amenable to testing at the scale of the current tests. The broader test series consisted of 7 tests. Due to continued data analysis

and paper length constraints,, this report focuses on the results of Tests 5 and 6. Table 1 gives details regarding the materials for these two tests.

Table 1. Materials for the fire tests.

Parameter	Test 5	Test 6
Material Description	Body Armor	Strips
Manufacturer	Hercules	Hexcel
Epoxy	3506 resin	3501-6 resin
Fibers	AW370 woven carbon fibers	Woven carbon fibers
Mass	36.6 kg	39.3 kg
Est. SA/Vol ratio	2.0 cm^{-1}	9.2 cm^{-1}
Arrangement	Two racks	Crib

In Test 5, we arranged a series of thick panels on two metal plates with wires welded to them to maintain spacing. The panels were made of the same material, but varied slightly in shape. The edges were not consistent or smooth, with some residual epoxy over-flow of varying thicknesses throughout the panel edge. The plates were somewhat oval, with major dimensions of 20 and 33 cm. The plates were approximately 1.0 cm thick, and had a flat surface area of approximately 600 cm^2. A total of 40 plates were burned in the test. The total mass of the material was 36.6 kg (80.7 lbs), and the estimated surface area to volume ratio was 2.0 cm^{-1}. An illustration of the lay-up is found in Figure 1 along with a corresponding photograph of the set-up.

A. B.

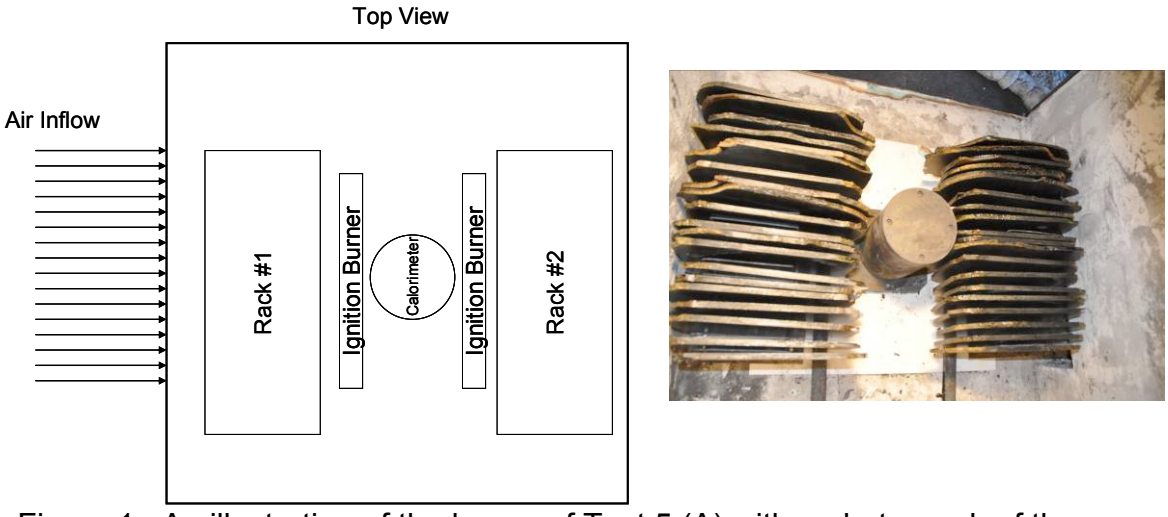

Figure 1. An illustration of the lay-up of Test 5 (A) with a photograph of the pre-test configuration (B).

In Test 6, we arranged 0.23 x 2.5 x 71 cm strips of material in a crib configuration. The lay-up of the crib is illustrated in Figure 2 with a sparse lower layer and a denser upper layer above the calorimeter. Total mass of the material was 39.3 kg (86.8 lbs), and the estimated surface area to volume ratio was 4-5 times higher than for Test 5, at 9.2 cm^{-1}. There were approximately 550-600 strips. Many of the strips were tapered at the edges, and there were a few (around 20) edge pieces that were

slightly shorter with irregular edges that were remnants of the cutting process. These pieces were placed at the top of the arrangement. Total height of the crib was approximately 50 cm, with the lowest 2/3 arranged as in Figure 2A and the top 1/3 as in Figure 2B.

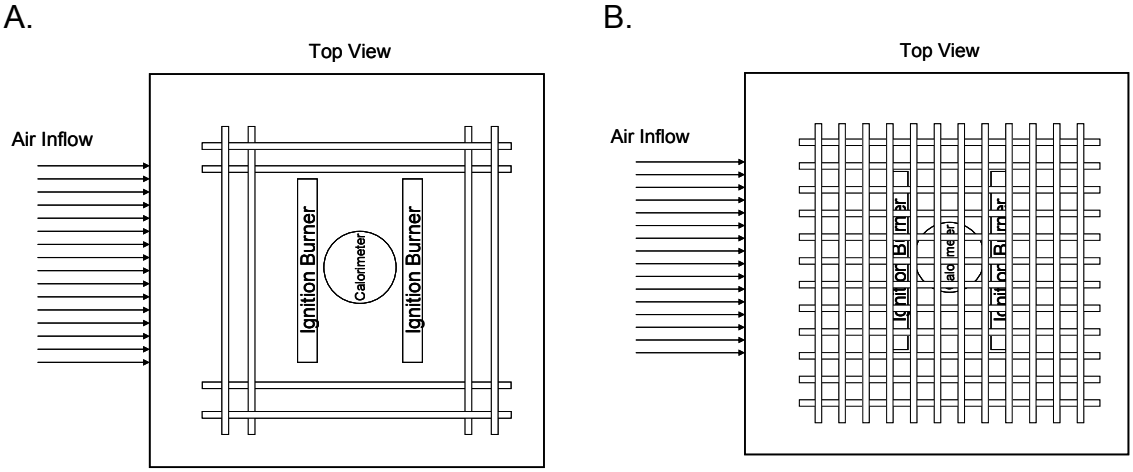

Figure 2. The lay-up of Test 6 showing (A) the lower-level lay-up and (B) the upper layer lay-up.

In each case, the crib and rack of material was placed on 5 cm high insulation blocks to provide clearance over the burners. The calorimeter was placed on the floor in the center of the enclosure. The gas burners were placed on either side of the calorimeter parallel to the duct flow inlet.

Test Enclosure

A 91 cm (3 foot) cubic enclosure (internal) was constructed to contain the materials for the test. A drawing of the enclosure and its assembly is found in Figure 3. At the base of the west wall, a 20.3 cm by 61.0 cm penetration was connected to a CFM™ TCC355 600 Watt blower. The top of the enclosure on the east end provided exhaust for the combustion products through a 20.3 x 66.0 cm hole. Two gas burners penetrated the north wall at the base to provide propane gas for a short duration until the test directors observed sustained flaming in the composite materials. Once the composite materials appeared to reach sustained combustion (typically 2-8 minutes), the gas burners were turned off and the remainder of the combustion was due to the chemical energy released from the composites. The steel enclosure was lined internally with Unifrax Durabord 3000 insulation, providing a low manufacturer specified thermal conductivity of 0.07 W/m-K at 315ºC.

Air inlet was controlled through the blower on the west side of the facility (Figures 1 and 2 are oriented with north being up as per standard map convention). The inlet was pre-characterized and set to give flow rates of approximately 0.24 m/s through the center of the 30 cm diameter ducts under cold conditions.

The test enclosure was located in the Sandia Igloo facility (9830) at the Lurance Canyon Burnsite. The full series of tests was conducted from January to March of 2011, and ambient temperatures were typically 0ºC at the beginning of each test.

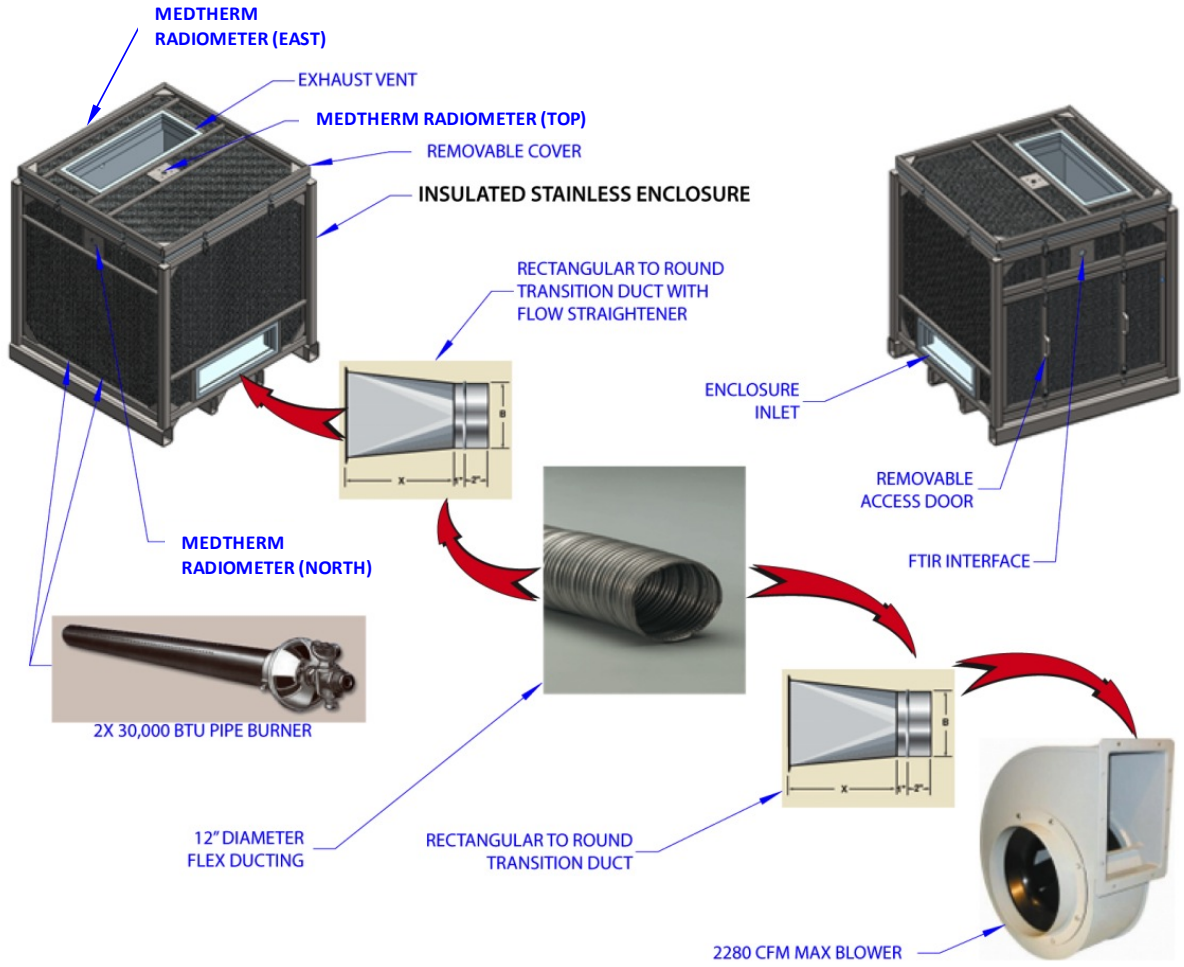

Figure 3. A schematic illustrating the test enclosure.

FTIR

A Midac I-Series 2001 FTIR was used to analyze the gases coming from the burning composite samples. Arms (3.8 cm diameter) extended from the IR source to a viewing position (or viewing line) above the exhaust of the burn box. Each arm elbow had a reflective mirror which reflected the IR signal from the source through one arm configuration, through the view line (open to exhaust conditions), through the symmetric/opposite arm configuration, to the detector. This configuration allows for an in situ measurement of the combustion gases, rather than a pump-drawn sampling line which can be prone to condensation of the hot gases. The arms were positioned 5 cm above and 5 cm outside the 20.3 cm × 66 cm rectangular exhaust, which allowed for a viewing line of approximately 76.2 cm. Prior to each test, the arms were aligned to obtain the highest signal intensity. Continuous samples were acquired once every 10.20 s and spectral curves were produced by triangular apodization. A schematic of the layout is found in Figure 4.

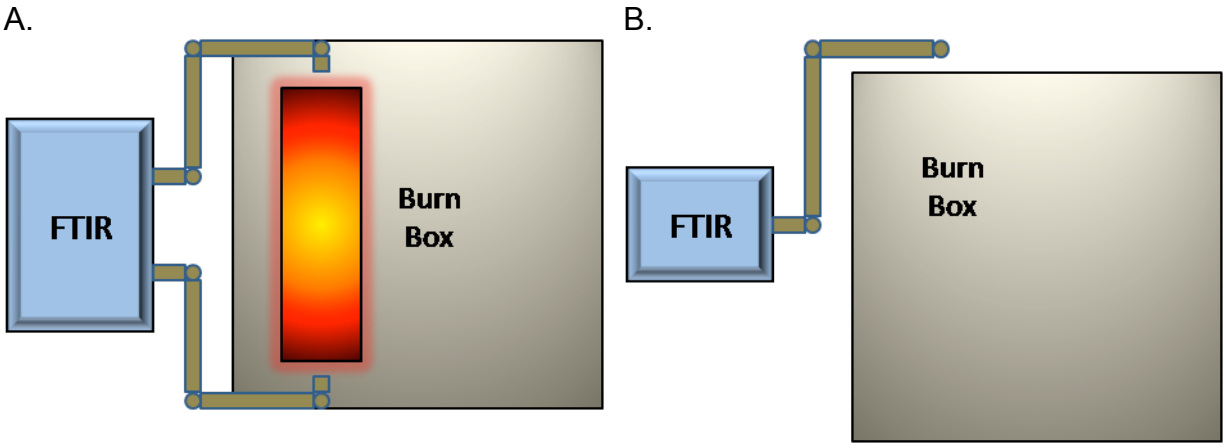

Figure 4. Schematic (A. top-view and B. side-view) showing FTIR arm configuration over the exhaust of the burn box.

Radiometers

Medtherm narrow-angle (5º) water-cooled, gas-purged, fast response thermopile radiometers (model P/N NVRW(ZnSe)-FTP-5.5-96-21248) were located near the top of the enclosure looking across the upper layer (labeled EAST and NORTH). An identical radiometer was located at the center of the top surface (labled TOP), oriented to look down at the calorimeter and crib. Radiometers were factory calibrated to the appropriate standards (ANSI/NCSL Z540-1 and ISO/IEC 17025). These were pre- and post-calibrated, and used to assess the radiation intensity in the exhaust layer at the top of the enclosure. The positions of the radiometers are shown in Figure 3. These radiometers have an advertised uncertainty of +/- 3%, but are known to have higher uncertainties, as much as 30% when exposed to significant convection.

Calorimetry

A bulk calorimeter was located on the ground in the middle of the enclosure. The calorimeter was constructed from 2.54 cm thick and of 15.24 cm external diameter Inconel® 600 tubing. End plates were 20 cm apart, and four thermocouples were welded to the internal surface at 90º intervals, and alternated circumferentially between 14 cm height above the base (pictured) and 6.4 cm above the base. The end plates were 2.54 cm thick. The internal portion was packed with Zircar 99 board insulation. The type K thermocouples provided data on the behavior of a solid body in response to the test environment. Type K thermocouples have a standard uncertainty of 0.75% of the reading in the range of 400-1300ºC. Composite materials were located around the calorimeter. A diagonal cut-away of the calorimeter is shown in Figure 5.

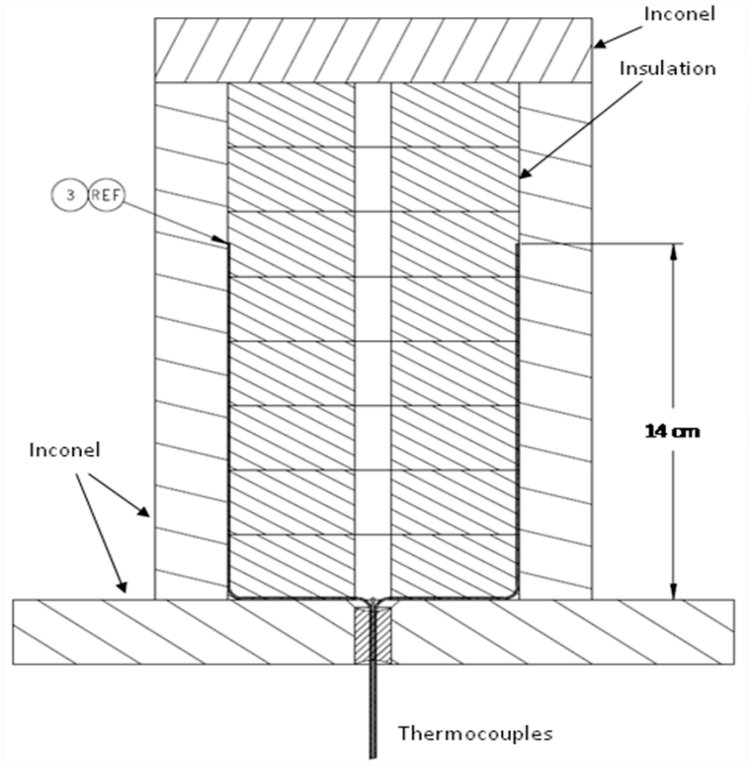

Figure 5. A cross-section cut-away drawing of the calorimeter.

Table 2 lists the thermocouple number along with a description of the location of the thermocouple during all the tests. The air inlet was on the west side of the facility for orientation purposes, as illustrated in Figures 1 and 2.

Table 2. A listing of the calorimeter thermocouples for the tests.

Thermocouple	Location	Height Above Top of Base (cm)
Cal 1	Southwest	6.4
Cal 2	Northeast	6.4
Cal 3	Southeast	14
Cal 4	Northwest	14

Other Instrumentation

In addition to the above described instrumentation, we fielded a Pitot based velocity probe to provide an indication of the velocity at the exit of the enclosure. The enclosure was instrumented with thermocouples to monitor the temperature of the instrumentation, structure, and insulation. An air-purged pneumatically aspirated matrix deposition sample holder was located above the flame to collect particulate samples in the plume. A residual gas analyzer was used to examine gaseous products through a sample tube located just below the Pitot based velocity probe. Videography was fielded for each test with three camera views focused on the exhaust port looking into the enclosure from above, and one camera positioned to capture the flaming by looking horizontally at the enclosure from a distance. We are still analyzing some of this data and as a result are not including it in the current paper.

Results and Discussion

Tests 5 and 6 were characterized by 20-40 minutes of flaming combustion, due primarily to the volatiles released from the pyrolysis of the epoxy. After flaming subsided, there was an extended 4-8 hour period over which a glowing combustion of the char and carbon fibers occurred. During early ignition, the flames could be seen growing in the enclosure and spreading to encompass the materials. As the intensity increased, the flames and smoke obscured the view into the enclosure. Once active flaming subsided, a clear view of the interior of the enclosure could be seen by the cameras.

Thermal Environment

Figure 6 and 7 show measured radiative fluxes (uncorrected) and calorimeter temperatures for Test 5. The flaming combustion took place in two phases, which may have corresponded to the ignition of one and subsequently the other rack.

This was a difficult test to ignite, presumably due to the thickness of the panels. After about six minutes, the flames were visually observed to be significant enough beyond the initial flaming of the gas burners that the gas burners were shut off. Heat fluxes were moderate until around 15 minutes. At that point, there was a significant increase in the heat flux, presumably due to more complete ignition across both racks of composite material. Between 15 and 30 minutes, there was a fairly steady environment in the enclosure, with heat fluxes from the radiometers being relatively constant and the calorimeter thermocouples showing a steady increase in temperature. A little past 30 minutes, there was an abrupt transition in the slope of the increase in temperature of the calorimeter thermocouples and in the measured heat fluxes from the radiometers. This corresponded with a transition from flaming combustion to glowing surface oxidation. Temperatures from the calorimeter peaked around 900ºC at 120 minutes and heat fluxes peaked slightly sooner at 100 minutes. Up until about 2 hours, the calorimeter temperatures show mostly consistent trending with each other. At approximately 2 hours, the calorimeter traces begin to diverge from one another. This is likely due to collapse of the materials around the calorimeter, resulting in a shift in the local environment near the surface of the calorimeter. After peaking around 1.5 hours, there was a slow decrease in radiometer readings over the next 3+ hours. During this time, the videos showed active glowing, suggestive of continued surface reactions through that time period.

Post-test calibrations of the radiometers were performed after the entire test series was completed to provide confidence in the results. Even though the radiometers were aspirated and cooled, the performance decreased by 20% (north), 25% (east), and 40% (top) from the original calibration by the end of Test 7. It is thought that the shift occurred in early tests (after Test 1 or Test 2) and was not a gradual bias across the tests because of the similarity in trending in the output from the radiometers from Test 1 through Test 7. These measured bias values have been used to correct the measured fluxes, and the corrected radiometer data are presented in Figure 8. Uncertainty in the measurements due to instrumentation uncertainty has not been incorporated into Figure 8 at this time.

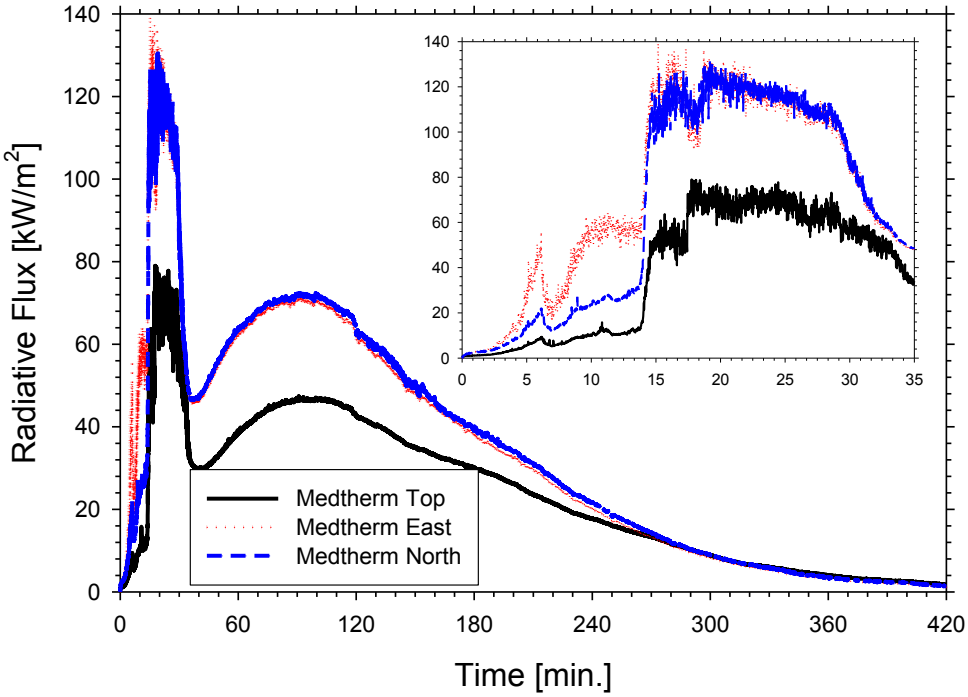

Figure 6. Test 5 uncorrected radiometer measurements. The inset graph shows increased resolution of the measured fluxes at early times.

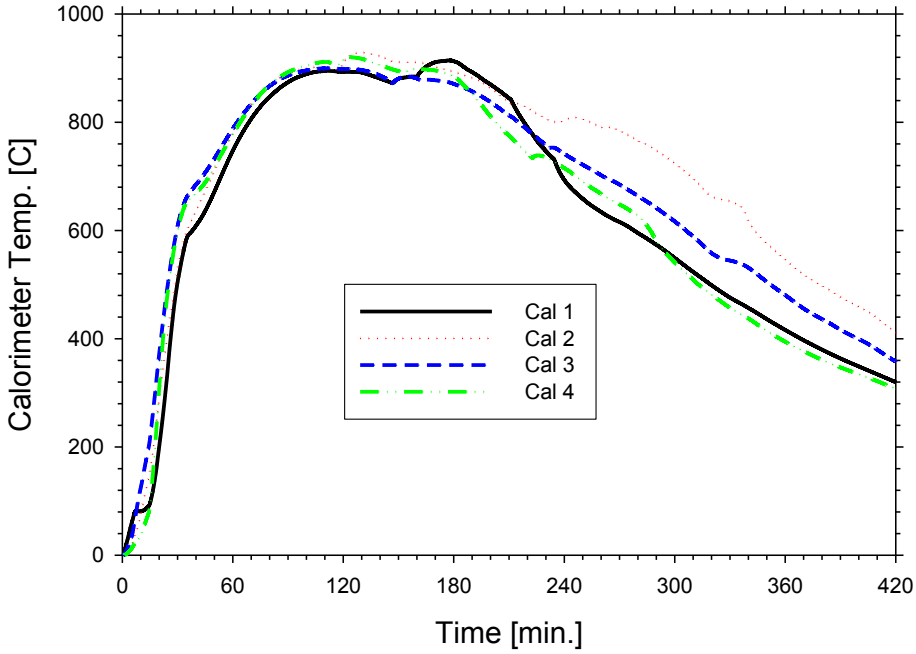

Figure 7. Test 5 calorimeter temperatures.

Also presented in Figure 8 is an analysis of the total flux incident to the calorimeter. The total flux incident the calorimeter was obtained based on an energy balance at the calorimeter surface which approximates all measured thermal increase as being due to radiation:

$$\varepsilon q_{itotal} = q_{abs} + \varepsilon q_{emit.} \quad (1)$$

In this equation, q is a heat flux, ε is the surface emissivity, and the subscripts *itotal*, *abs*, and *emit*. are for total incident, absorbed, and emitted flux respectively. The absorbed flux is obtained using a lumped capacitance approximation:

$$q_{abs} = \rho CpL \frac{dT}{dt} \tag{2}$$

In this equation, ρ is the density, *Cp* is the specific heat, *dT* is the temperature change over the time interval *dt*, and *L* is the thickness of the calorimeter. The re-emitted term is calculated as if the calorimeter were isothermal:

$$q_{emit.} = \sigma T_{Cal}^4 \tag{3}$$

In this equation, σ is the Stefan-Boltzman constant, and T_{Cal} is the average calorimeter temperature as measured by the thermocouples. This model neglects the conduction of the Inconel®, which was found to be a reasonable assumption after comparing results of this methodology with a more detailed methodology in an inverse code that accounts for conduction through the Inconel®. In addition, convection is not included this analysis. For the analysis, mean physical properties were employed as detailed in Table 3. Absorptivity and emissivity are also assumed to be equal.

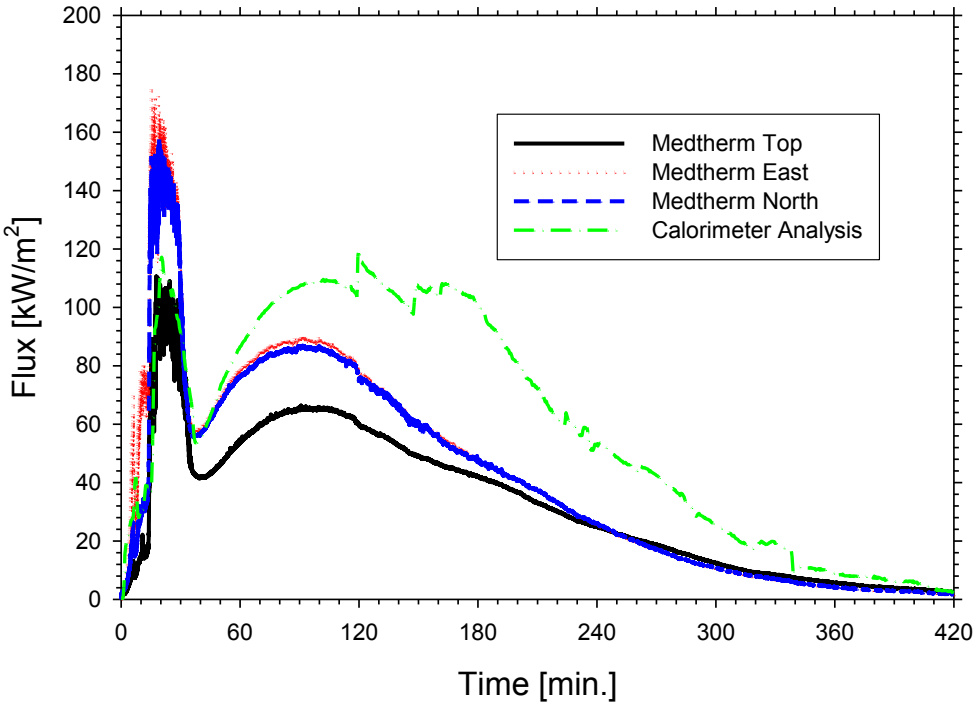

Figure 8. Test 5 corrected radiometer measurements with mean total flux derived from the analytical model based on the calorimeter temperatures.

Table 3. Assumed Properties for the Thermal Model

Property	**Units**	**Value**
Inconel Density	kg/m^3	8430
Inconel Specific Heat	J/kgK	540
Surface Emissivity		0.6

In comparing the calculated value of total flux incident on the calorimeter and the heat flux gauge measurements as shown in Figure 8 both show an increase in heat flux during flaming combustion, followed by a decrease and subsequent increase in heat flux when the combustion regime changes from flaming combustion to glowing combustion. Quantitatively, the calculated value of total heat flux incident on the calorimeter and the heat flux gauge measurements are in moderate agreement. As the radiometers and calorimeter were focused at different locations, some differences are naturally expected. Peak fluxes during the flaming combustion range from 90-170 kW/m^2, and peak fluxes during the glowing combustion range from 60-120 kW/m^2.

Figure 9. Test 5 video frames at regular half-hour intervals as time-stamped.

Figure 9 shows frames at half-hour intervals as captured by video during the test. On the left of the images, one of the composite pieces fell early in the test and is lying at approximately 90º orientation to the rest of the pieces in good view of the cameras. It is almost completely consumed by the 2 hour mark. It should be noted that this piece was located in the rack that was nearest the air inlet. This and its orientation likely played a significant role in its apparent early consumption compared to the other pieces on the same rack and those on the other rack.

Figure 10 shows two photographs taken beyond four hours into the test that illustrate the west rack (Rack #1) was consumed before the east rack. These photographs also show material lying against the calorimeter, supporting the assumption that a shift in material location caused a divergence of the calorimeter temperatures. The residual material was collected and weighed, and revealed that 97.3% of the material was consumed in the test. Most of the residual material was light and pliable, suggestive of fibers that had not fully consumed. There were some pieces that were still somewhat rigid and thick, albeit smaller and less dense than the original material. The residual strength is presumably due to the formation of char during the epoxy decomposition. After hours immersed in the thermal environment of the test, it is unlikely that these pieces contain epoxy that had not undergone some kind of thermal decomposition. A more complete analysis of these residues remains for future work.

Figure 10. Test 5 photographs of the late-test burnout. The left photograph shows the east rack still glowing strongly, while the western rack near the air inlet is mostly consumed. The right photograph shows a similar view at a later time. Air enters from the left in these photographs.

Figure 11 and 12 show measured uncorrected radiative fluxes and calorimeter temperatures for Test 6. This test was much easier to ignite than Test 5. This is probably due to the significantly increased surface area of the composite material and potentially due to improved ventilation through the crib compared to the racks. After two minutes of the gaseous burn time, there was enough independent burning that the gas burners were turned off. The flaming combustion time period was about 50% shorter than that for Test 5. After 20 minutes, there was a significant decrease in the heat flux. This corresponded to a minor inflection in the calorimeter thermocouple temperatures and a large drop in the measured heat fluxes from the radiometers. This marked the transition from flaming combustion to glowing surface oxidation. Temperatures from the calorimeter and heat fluxes from the radiometers both reached peak values at approximately 60 minutes. Peak calorimeter

temperatures were approximately 1000ºC, 100ºC higher than in Test 5. Calorimeter temperature trends were very consistent, different from Test 5. This is attributable to the crib remaining more rigid than the panels in the Test 5 configuration. After peaking around 1 hour, there was a slow decrease in radiometer readings over the next 3+ hours. During this time, the videos showed active glowing combustion.

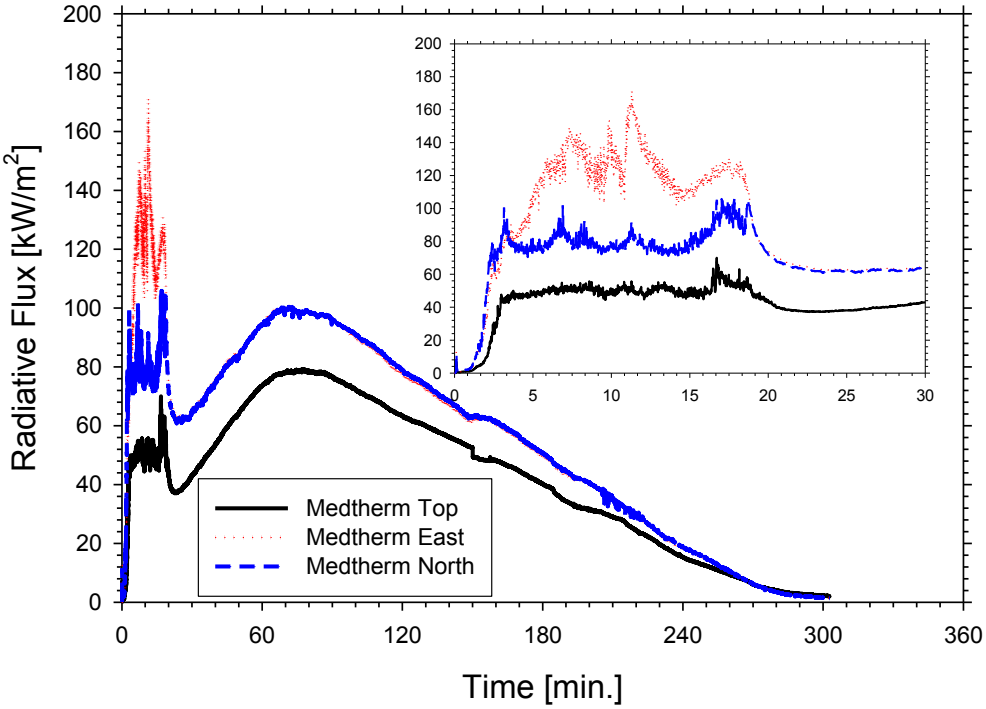

Figure 11. Test 6 uncorrected radiometer measurements. The inset graph shows increased resolution of the measured fluxes at early times.

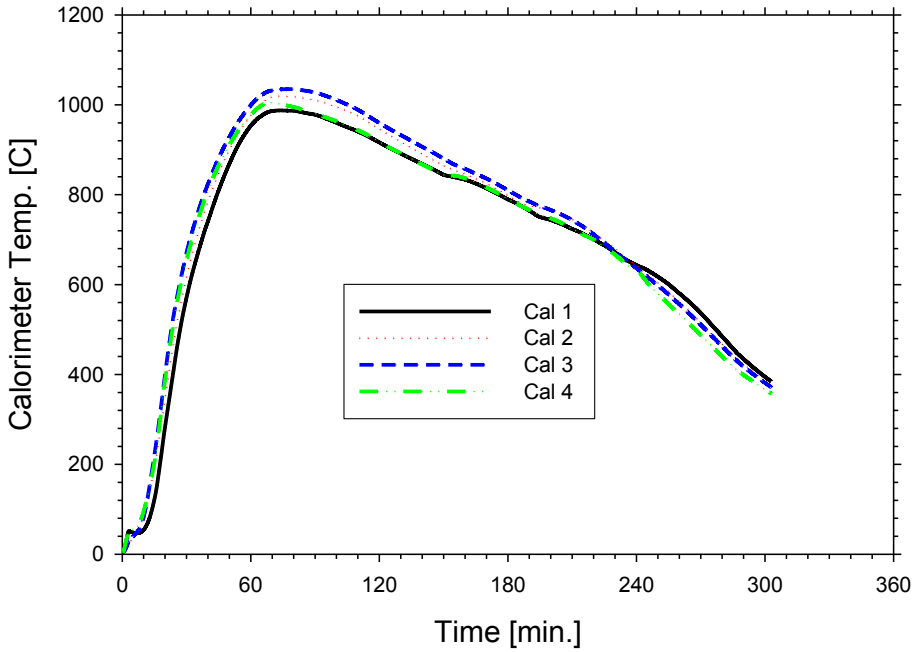

Figure 12. Test 6 calorimeter temperatures.

An identical methodology was used for correcting Test 6 results and analyzing the calorimeter temperatures to deduce the total incident flux to the calorimeter as was used for Test 5. Figure 13 illustrates those results. Peak heat fluxes during the flaming combustion varied between 80-200 kW/m^2, while the glowing combustion heat flux peaks were more narrowly distributed from 110-160 kW/m^2. Flux measurements during the flaming regime for Test 6 compared with Test 5 were not discernibly different from a general standpoint, but there were some specific differences in the predicted magnitudes of the individual gauges. Peak heat fluxes during the glowing combustion phase were significantly higher in Test 6.

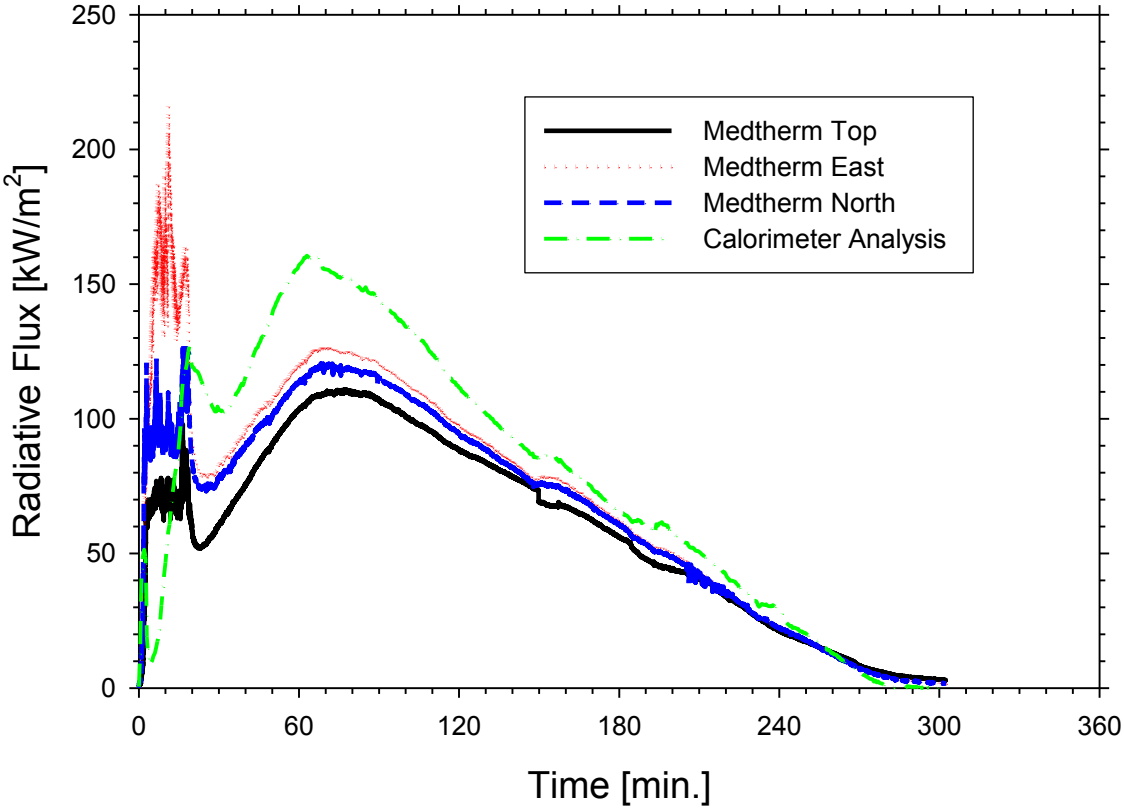

Figure 13. Test 6 corrected radiometer measurements with mean total flux derived from the analytical model based on the calorimeter temperatures.

Figure 14 shows still frames from a video of the test taken at half-hour intervals. Some interesting observations can be made from these stills. First, the material appears to be glowing with increased intensity on the internal parts of the crib compared to the external. The crib also appears to consume preferentially from the more central material upward. The increased glowing and increased consumption rate in the interior of the domain could be related to an increase in oxygen in the center region of the crib due to the inlet air availability and to the radiative loss of energy to the external portions of the crib and the external surroundings. From the images and videos, it is difficult to identify independent decomposition of the individual strips; instead, the decomposition and recession of material appears to behave as if the crib is a uniform solid structure. This may be suggestive of interaction between the strips during early decomposition. Composites are known to swell and a char layer forms as they decompose, which could be a contributing mechanism to this observation. The swelling and char formation at the locations

were the strips are in contact with one another, could be causing cohesion and thus some structural integrity at these locations. In the 1:30:00 frame and the 2:00:00 frame, there is necking of the strips when compared to the contact locations where the strips cross each other. This is suggestive of the importance of the oxygen availability and ventilation to the consumption rate of the material. Video of the event does not suggest small pieces individually falling. When movement occurred in the crib, it was typically a shift of the entire structure together. The first of such shifts was recorded at 3:25:10, after which they occurred more frequently.

Figure 14. Test 6 video frames at regular half-hour intervals as time-stamped.

The post-test composite residual material was weighed and found to be 6.7% of the original material mass, or a mass loss of 93.3%. Figure 15 shows photographs of the final glowing combustion and of the final appearance of the crib. Curiously, the

majority of material and glowing is found near the air inlet, while the regions away from the air inlet show more sparse material. It is impossible to guarantee that the collapse of the crib happened vertically and that the distributions in Figure 13 were not caused by relocation during the collapse. But it is probable that the material as distributed is representative of the regional burnout, and that contrary to Test 5 results, the material furthest from the air inlet was preferentially consumed.

Figure 15. Test 6 photographs of the late-test burnout. The left photograph shows minor glowing in several regions of the collapsed crib. The right photograph shows a similar view at a later time. Air enters from the top of these photographs.

The residual materials are interesting to examine. As is evident in the photographs, some of the principal structural forms were still discernable in the residue. A comparatively substantial amount of material remained at or near the contact locations where the strips cross one another. Based on post test observation it appears that the strips had fused together at the contact locations and were not easy to separate as was the case prior to the test. These formed thick block-like structures with remnants of partially consumed strips protruding from the blocks. There was no evidence of a similar cohesion for the strips that were not contact in the initial crib set-up. This suggests that the apparent cohesion of the strips is most likely caused by a fusing of contacted materials through the char formation in the contact locations. The gaps between strips are probably not visible at the resolution of the captured video, which explains why the individual strips are not seen in the video images. The crib is thought to have been held together by the cohesion at the contact points, thus resulting in an appearance of the originally separate material acting as a unit as opposed to having random failure locations.

Through both tests during the flaming combustion times, black solids were observed emitted from the exhaust hole. Some residues were captured and observed to be in form more consistent with large soot agglomerates than liberated fibers. They were not rigid or linear like the fibers, rather they smudged and deformed when pressed between the fingers. The propensity of burning epoxy to form soot is expectedly high because of the aromatic rings in the un-burnt epoxy chemistry. Typical epoxies have two aromatic rings in their monomer formula. This provides a shortcut to forming soot when compared to most traditional gas and liquid hydrocarbon fuels. Soot is primarily aromatic carbon. The fibers were not observed either during the test or afterwards by examining the surroundings to become airborne and create a respiratory hazard. Both Test 5 and 6 materials were woven fabrics, which may help ameliorate the hazard.

Combustion Products

FTIR

The spectral adsorption curves obtained over time were compared to four standard gas curves, namely H_2O, CO_2, CO, and CH_4. Assuming that the adsorption of the gas is linear with respect to its concentration and pathlength, the combustion products were characterized by weighting the four standard gas curves to correspond to the actual test curve. For the analysis in this paper, a constant product gas temperature of 500ºC was assumed. A comparison of test results to the combined standard curve is shown in Figure 16, showing some of the characteristic adsorption bands, though some are not observed in this curve (e.g. CO, CH_4). A non-linear solver was used to determine proportions of each combustion gas, and overall concentrations were calculated.

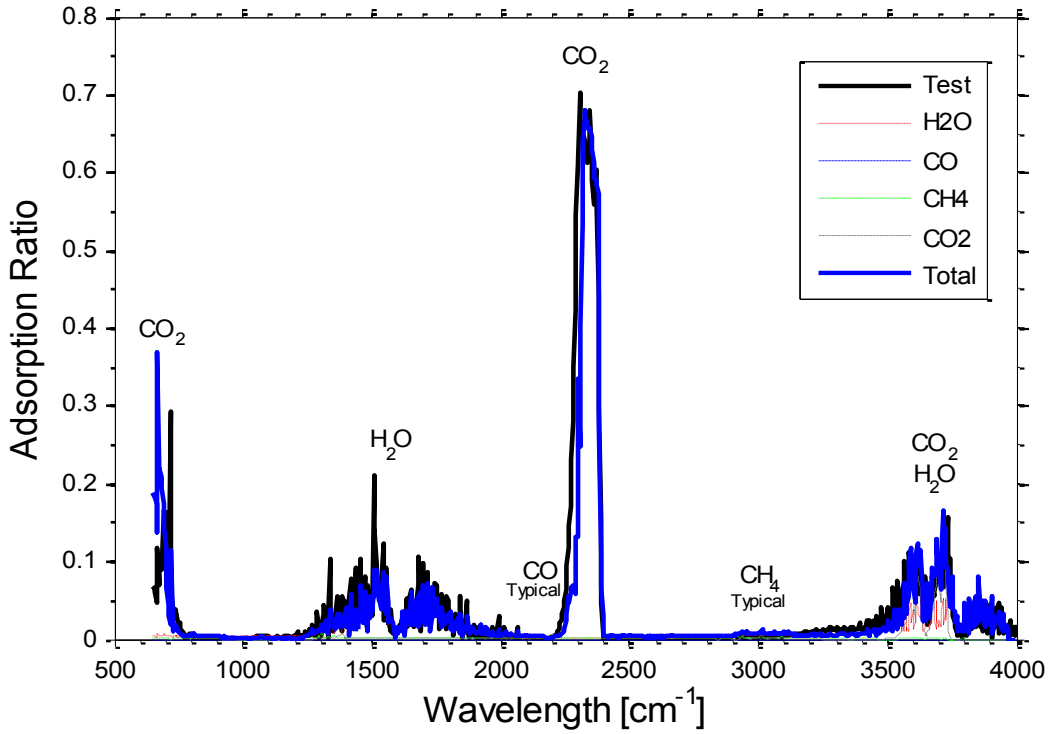

Figure 16. Spectral adsorption curves comparing the FTIR test to the weighted standard gas species.

Turbulence during the test, particularly during flaming combustion, generated significant noise for the FTIR measurements. Some of this noise can be seen in the displacement of some adsorption bands, particularly the CO_2 (2200-2400 cm^{-1}) and H_2O (3100-3500 cm^{-1}) shifting to a lower wavelength as shown in Figure 17.

Due to experimental problems during Test 6, FTIR data was not available. Concentration results are shown in Figure 18 for Test 5. As consistent with flaming combustion, flammable species (CH_4, CO) appeared to spike and then smooth out as the flame extinguished. Also, as consistent with char oxidation, levels of CO gradually increased then began to decline as oxidation ceased. Small amounts of H_2O were also observed during pyrolysis combustion, presumed to be from the hydrocarbons (particularly the source H atoms) emitted from the burning resin matrix.

That signal is not present during the glowing combustion phase, because the primary reactants are carbon and oxygen.

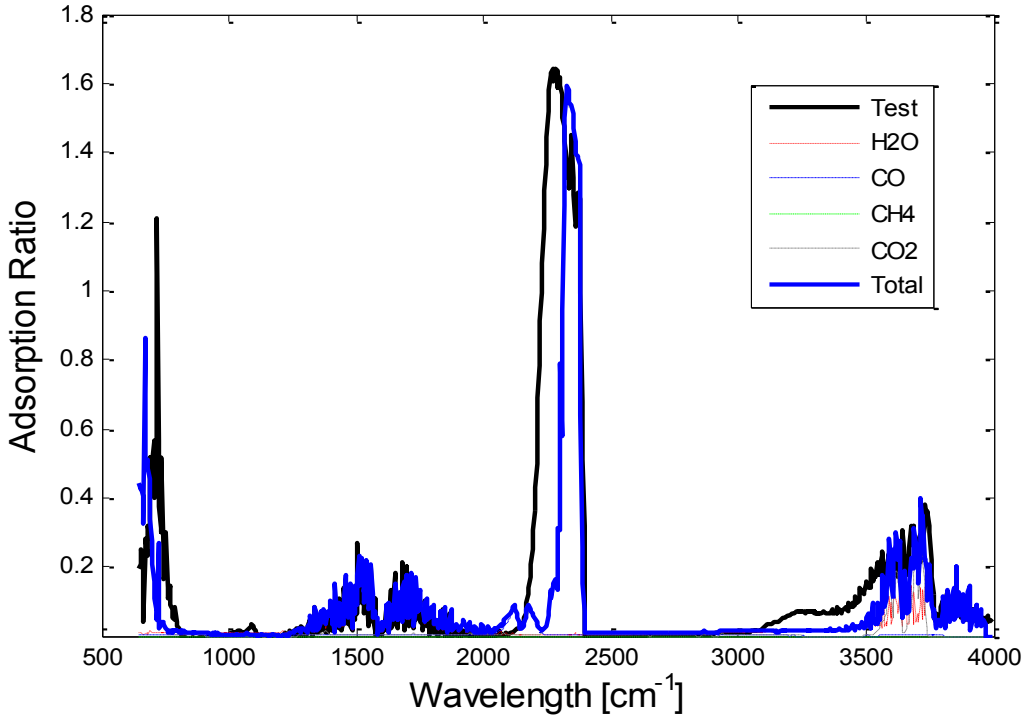

Figure 17. Characteristic stretching of spectrum during the most active turbulent regime of combustion.

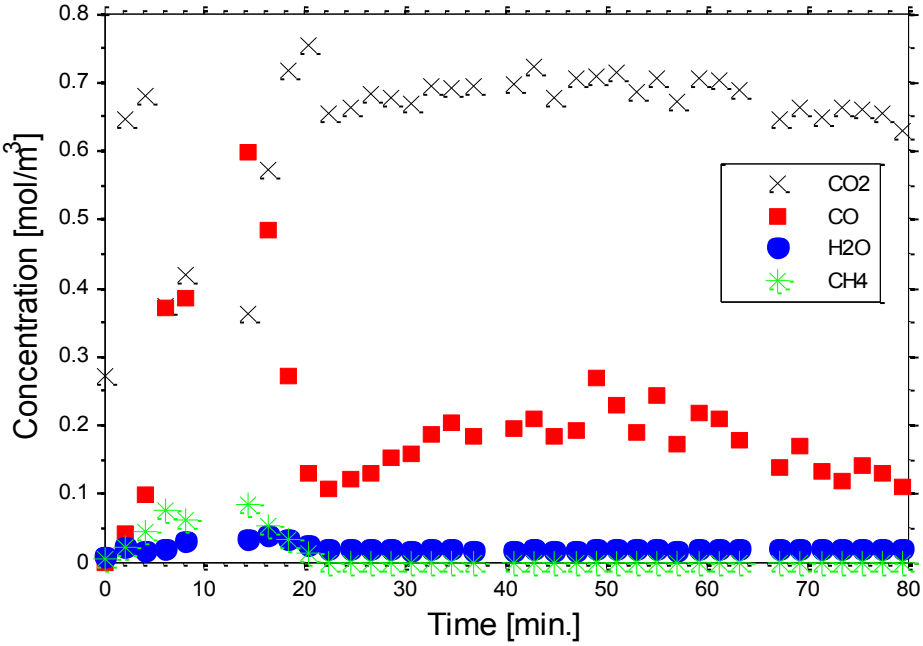

Figure 18. Test 5 concentrations derived from FTIR measurements. The short data gap occurring at the 10 min time location resulted from interferences in the FTIR data during the strongest combustion phase.

General Discussion

Although these tests are not a perfect analog to an aircraft fire, they are intermediate-scale tests that can be used to infer behavior that bridges from some of the more common small-scale data to larger-scales. Since performance data for composite fires at larger scales are scarce, these data are believed to be valuable.

An aircraft fire from primarily aluminum framed aircraft will be caused mostly by the aviation fuel. For a runway spill or a remote crash condition, this is normally the dominant source for fuel. Absent suppression, jet fuel will burn with a high intensity for a moderate period of time, typically on the order of 30 minutes. This can be extended if there is a porous ground, an enclosure, or a depression that creates a deep pool. Direct flaming regions are sufficiently hot to cause aluminum to melt, potentially aiding in the exposure of internal contents of the aircraft to the fire [Suo-Anttila and Gritzo, 2001, Lopez et al., 2010]. The behavior of the composites in this test suggest that there is a good probability that thermal release for a composite aircraft fire on a composite-framed aircraft can take place over a much longer time period.

These tests suggest that there is a likelihood of a significantly different mode of burning that can occur when carbon fiber based composites are a significant portion of an airframe. Composites alone are moderately flammable once ignited, and even without significant external fuel can sustain combustion. Flaming combustion lasted approximately 30 minutes for the thicker composite pieces in these tests, and around 20 minutes for the thinner materials. Real aircraft are much more massive with a range of thicknesses, and can therefore be expected to combust in a flaming mode for a longer period of time due to the increased mass of material. They are also longer in length, and in a fire there will probably be varying degrees to which the composites are exposed to a ground fuel fire. Less exposed parts of an airframe may not burn at all, or require time for flame spread to occur, extending the duration. Flame spread may be more relevant for a large aircraft on fire. Glowing combustion of the fibers requires oxygen, which may be scarce at early times in the event of a large pool fire. It is probable that the burn time for the fibers in a fire with more material will also be different because real aircraft are unlikely to experience adiabatic surroundings as in these tests.

While burn times are important, the intensity of the burn is also important. Because of the way the tests were designed in a well insulated box, we believe that the data provide higher heat fluxes compared to an average open fire scenario. Heat flux measurements showed much higher readings during the flaming combustion phase of the experiment, with peak fluxes ranging from 80-200 kW/m^2. During the glowing combustion phase, lower heat fluxes were obtained, with peak measured fluxes ranging from 60-160 kW/m^2. Peak radiation from the flaming combustion was found in the gases in the upper layer of the test enclosure. During glowing combustion, peak fluxes were obtained from the calorimeter which was located close to the composite material. Peak calorimeter temperatures were in the 900-1000 ºC range for both tests. This is suggestive of fluxes in the 100-150 kW/m^2 range based on a radiation analogy calculation, and shows consistency with the fluxes measured by the radiometers in the upper layer and the extracted calorimeter fluxes from the model.

Residual composite material masses were very low, and morphology suggests that they were a result of the thermal environment dropping below the temperature required for sustained glowing combustion. Because of the insulated design of the test chamber, the materials were placed in a fairly idealized environment for maximizing consumption. Under a less ideal scenario, we speculate that there might be more residual mass. We believe, and thermogravimetric analysis supports the theory that there is very little material that cannot be consumed with the correct environmental conditions. We found that even in an intense environment that the materials will hold together absent a strong external force. This is consistent with some previous work [Lopez et al., 2011] where a ¼ scale carbon fiber epoxy fuselage was found to provide radiative shielding long after an aluminum frame would melt away.

We believe that pieces of the composite structure fused together during the fire possibly during char formation, which although weakened, provided sufficient strength to keep pieces of the crib together through the burn. Residual strength is probably due to char material formed from adhesion created early in the burn process. This phenomenon has not been previously reported to our knowledge, and may be an important phenomenon to recognize when responding to a fire. Closely mated parts such as hatch openings may require unexpectedly high amounts of force to open in the post-fire environment.

The FTIR was unable to extract reliable signal during the most severe flaming portion of the tests. Longer wavelength signals can often traverse optically opaque flames. The problem in this test was likely a combination of smoke obscuration and glowing emission obscuration. Trending before and after the heavy flaming is suggestive of how species emission was evolving when signals were not obtained. H_2O and CH_4 both peaked during the flaming combustion phase, suggestive of hydrocarbon burnout. They both decreased back to initial baseline values during the glowing combustion phase where emitted gases are expected to be mostly CO and CO_2 from the carbon fibers. The CO and CO_2 also trended as expected. The initial low CO_2 increased promptly and stayed high for the duration of the test. CO trended high during the flaming combustion period, and showed a trend similar to the heat fluxes through the glowing combustion phase. The excess CO is most likely due to the CO produced during the carbon fiber oxidation that has not been converted to CO_2.

These tests contribute to the range of tests already existing for composite material fires. Tests were designed to scope the peak thermal environment possible from carbon fiber epoxy materials. The low air flow rate and insulated nature of the box was an attempt to create an extreme environment compared to a more open environment test of similar materials. The peak heat fluxes measured during flaming ranged between 80 kW/m^2 and 200 kW/m^2, which are lower than peak heat fluxes measured in a liquid hydrocarbon fire. For comparison, Suo-Anttila and Gritzo [2001] show peak fluxes from a liquid hydrocarbon fire, around 400 kW/m^2. One cannot conclude that a composite material fire results in lower heat fluxes than in a liquid hydrocarbon fuel fire because larger scale composite fires may experience similar phenomena characteristic of a high heat flux fuel fire. In this test series, the burn times were very long. This suggests that the severity of a composite fire may be more unique in terms of duration and less because of the intensity of the reactions.

Unsuppressed, the char and fibers from the composite were found to burn for 5-8 hours. Real scenarios could result in even longer events.

Conclusions

The composite tests detailed in this report provide new and unique data at an intermediate scale on the combustion behavior of composites. The tests were designed to be thermally severe, and representative of an extreme fire environment. Principal findings suggest:

- A flaming region of 20-30 minutes followed by 5-8 hours of glowing surface oxidation reactions.
- Flaming combustion heat fluxes from the radiometers range from 80 kW/m^2 to 200 kW/m^2.
- Glowing combustion heat fluxes range from 60 kW/m^2 to160 kW/m^2 from the radiometers, and calorimeter data suggests peak fluxes in the 100 kW/m^2 to 150 kW/m^2 range.
- Under idealized fire conditions it is possible to get high burnout of the composite material.
- Adjoining materials may adhere to each other, probably due to char formation during decomposition. After volatiles are driven off, there still appears to be residual strength in the char structure.
- Significant CO is emitted during flaming and glowing combustion phases. Copious amounts of soot are formed during flaming combustion, representing two of the main chemical hazards.

Acknowledgements

The authors are grateful for the hard work of the technologists who contributed significantly to the experimental test team at Sandia National Labs, which includes Sylvia Gomez, Ciro Ramirez, Bennie Belone, Randy Foster, and Richard Simpson. Also to Richard Streit for help with the enclosure design. Also to the internal programs for supporting the work.

Sandia National Laboratories is a multi-program laboratory managed and operated by Sandia Corporation, a wholly owned subsidiary of Lockheed Martin Corporation, for the U.S. Department of Energy's National Nuclear Security Administration under contract DE-AC04-94AL85000.

References

Babrauskas, V., Ignition Handbook, Fire Science Publishers, 2003.

Brown, J. E., E. Braun, W. H, Twilley, “Cone Calorimeter Evaluation of the Flammability of Composite Materials,” National Bureau of Standards, NBSIR 88-3733, March 1988.

Delfa, G.L., J. Luinge, A. G. Gibson, “Next Generation Composite Aircraft Fuselage Materials under Post-crash Fire Conditions,” Engineering Against Fracture: Proceedings of the 1st Conference, 2009, pp. 169-181.

Fanucci, J.P., “Thermal Response of Radiantly Heated Kevlar and Graphite/Epoxy Composites,” Journal of Composite Materials, Vol 21, 1987, p129-139.

Hubbard, J.A., A.L. Brown, A.B. Dodd, S. Gomez-Vasquez, and C.J. Ramirez, “Aircraft carbon fiber composite characterization in adverse thermal environments: radiant heat and piloted ignition flame spread,” Sandia Report SAND2011-xxxx In preparation.

Jiang, G., S. J. Pickering, G. S. Walker, N. Bowering, K.H.Wong, C. D. Rudd, “Soft ionisation analysis of evolved gases for oxidative decomposition of an epoxy resin/carbon fibre composite,” Thermochimica Acta V., 454, 2007, pp. 109-115.

Levchik, S. and E. D. Weil, “Review: Thermal decomposition, combustion and flame-retardancy of epoxy resins- a review of the recent literature,” Polymer International, V. 53, 2004 p. 1901-1029.

Lopez de Santiago, I., I. Saez de Ocariz Granja, A. Arbildi Fernandez, F. Fernandez Sanchez, A. Cortes Rueda, and K. Fernandez Horcajo, “Fire Penetration in a Aircraft Made in Composite,” from the International Congress: Combustion and Fire Dynamics, Univeridad de Cantabria, Santander, Spain, 20-23 October, 2010, pp. 389-407.

Makino, A., T. Namikiri, and K. Kimura, “Combustion rates of graphite rods in the forward stagnation field with high-temperature airflow,” Combustion and Flame 132, pp. 643-753, 2003.

Mouritz, A. P., “Fire Safety of Advanced Composites for Aircraft,” ATSB Research and Analysis Report B2004/0046, Australian Transport Safety Bureau, April 2006. ISBN 1 1921092432.

Quintiere, J.G., Walters, R. N. and Crowley, S., “Flammability Properties of Aircraft Carbon-Fiber Structural Composite,” 2007, U.S. Department of Transportation, Federal Aviation Administration: Washington, DC. pp. 1-34.

Suo-Anttila, J.M. and Gritzo, L.A., “Thermal Measurements from a Series of Tests with a Large Cylindrical Calorimeter on the Leeward Edge of a JP-8 Pool Fire in Cross-Flow,” Sandia report SAND 2001-1986, July 2001.

Tyson, J.H., J. Childress, J.S. Fontenot, G.L. Wildman, “Carrier-Deck Fire Response of Graphite Epoxy Composite Materials,” NWC Technical Publication 6713, Naval Weapons Center, China Lake, CA, May 1986.